IOP Publishing Journal of Physics: Condensed Matter
J. Phys.: Condens. Matter **32** (2020) 284001 (12pp) https://doi.org/10.1088/1361-648X/ab7cc5

Soft mechano-chemistry of molecular hubs in mitotic spindle: biomechanics and mechanical proofreading at microtubule ends

Debashish Chowdhury[1] **and Dipanwita Ghanti**

Department of Physics, Indian Institute of Technology Kanpur, 208016, India

E-mail: debch@iitk.ac.in

Received 20 November 2019
Accepted for publication 5 March 2020
Published 15 April 2020

Abstract

A microtubule (MT) is a long stiff tube-shaped filament formed by a hierarchical organization of a large number of tubulin protein molecules. These filaments constitute a major structural component of the scaffold of a multi-component macromolecular machine called mitotic spindle. The plus ends of the MTs are tethered to some specific binding partners by molecular tethers while those of some others are crosslinked by crosslinking molecules. Because of the non-covalent binding involved in the tethering and crosslinking, the attachments formed are intrinsically 'soft'. These attachments are transient because these can get ruptured spontaneously by thermal fluctuations. By implementing *in silico* the standard protocols of *in vitro* molecular force spectroscopy, we compute the lifetimes of simple theoretical models of these attachments. The mean lifetime is essentially a mean first-passage time. The stability of cross-linked antiparallel MTs is shown to decrease monotonically with increasing tension, a characteristic of all 'slip-bonds'. This is in sharp contrast to the nonmonotonic variation of the mean lifetime with tension, a mechanical fingerprint of 'catch-bonds', displayed by the MTs tethered to two distinct binding partners. We mention plausible functional implications of these observations in the context of mechanical proofreading.

Keywords: first-passage time, microtubule, kinetochore, catch bond, molecular force spectroscopy, force clamp

(Some figures may appear in colour only in the online journal)

1. Introduction

Soft matter [1] are characterized by some noncovalent weak bonds; the corresponding bond energy is comparable to the typical thermal energy k_BT at room temperature where k_B denotes the Boltzmann constant. For example, the strength of a hydrogen bond is typically few tens of k_BT [2]. Therefore, spontaneous thermal fluctuations are sufficient for rupture of weak bonds. At room temperature $T \simeq 300$ K, $k_BT \simeq 4$ pN nm. Therefore, a force f that can perform work of the order of thermal energy causing a displacement of the order of 1 nm, is $f \simeq 4$ pN. Thus, externally applied tensions as weak as a few pN can rupture noncovalent bonds in soft matter. The weak bonds that shape the tertiary structure of a macromolecule can get easily ruptured by such small forces resulting in a change of its conformation. Similarly, breaking of weak bonds that hold two distinct macromolecules together can detach the two molecules from each other.

Many important structural joints formed by non-covalent bonding of the components of molecular machines in living cells perform key roles also in the biological function of those machines. In the last few years we have developed theoretical models for a few such specific joints in a molecular machine and studied the rupture of those joints by

[1] Author to whom any correspondence should be addressed.

mechanical forces [3–6]. In this paper we study a different molecular joint, in the same machine, whose force-induced rupture has not been modelled theoretically till now. However, in the spirit of this special issue of the journal, we present the model and results for this particular molecular joint from a broader perspective. We compare and contrast the main features of the new results with those reported in our earlier works [3–6] for some other molecular joints of the same multi-component molecular machine.

Numerous phenomena that are crucial for the survival of a living cell rely on the coupling between mechanical and chemical processes. On the one hand, the cell and its subcellular structures are often subjected to compressive and tensile forces, shear stress as well as hydrostatic pressure. Most often the mechanical stress is converted to a chemical signal which elicits response by activating the downstream processes. The reverse process, namely conversion of chemical energy into mechanical work is carried out by wide varieties of molecular motors [7, 8]. Here we study the mechano-chemistry of some key molecular joints [6, 9] in a multi-component molecular machine, called mitotic spindle [10, 11], that carries out mitosis, i.e., the segregation of replicated chromosomes before a cell divides into two daughter cells [12–14].

A mitotic spindle is a network of filamentous proteins, molecular motors and many other specialized non-motor proteins [15]. In the macroscopic world, we are familiar with scaffolds and networks made from solid beams, rods and struts. These elastic components of the network deform elastically when subjected to mechanical load. Many large-scale, complex networks are formed by connecting these elements by bolts and joints. At first sight, networks formed by proteinous filaments in a mitotic spindle may appear similar to macroscopic network of beams, struts and cables joined by nuts and bolts. But, this superficial similarity is quite deceptive. Not only the components of this network have a high rate of turnover, the scaffold self-organizes, its shape fluctuates strongly even in the steady state, and it can dynamically remodel its own architecture and, after completing chromosome segregation, is disappears completely. In this paper we highlight some of the important consequences of this extremely dynamic and transient nature of the microscopic natural scaffolding of a mitotic spindle.

One of the major species of filaments in the structural scaffold of a spindle is microtubule (MT) [16]. During the process of assembling a mitotic spindle, molecular joints are formed by the establishment of non-covalent bonds between MTs and their specific binding partners [18]. After serving its biological function as the segregator of the replicated chromosomes, a mitotic spindle disassembles. Therefore, most of the molecular joints linking MT with its binding partners in a mitotic spindle are deliberately designed to be transient. Even if not subjected to any externally applied tension such a bond survives only for a finite lifetime beyond which it gets ruptured spontaneously. The lifetime of such transient joints is the main quantity of interest in this paper.

Exploiting the unusual kinetics of their polymerization and depolymerization [17], the MTs themselves generate pushing and pulling forces. Moreover, the molecular motors in the spindle are also active force generators. Therefore, the transient joints formed by MTs with their binding partners must have the strength and stability to withstand the pushing and pulling forces till their biological functions are completed. Nevertheless, during the lifetime of the spindle, parts of a molecular joint can not only break but detached partners can again reattach. Thus, mechanical response of the joints in a spindle is dominated by inelastic mechanics [19] of fracture and rupture. It is this rupture kinetics that is the main theme of this work.

Molecular force spectroscopy (MFS) [20–24] probes various aspects of the rupture of ligand–receptor bonds. Almost a decade ago the experimental tools of MFS were first adapted for *in vitro* studies of molecular joints where MTs and their specific binding partners are held together by non-covalent bonds in a mitotic spindle. In the last few years we have developed stochastic kinetic models for studying the stability and strength of some of those molecular joints [3–6]. The protocols used in our computer simulations of those models are essentially *in silico* analogs of the common protocols of MFS for *in vitro* experiments on ligand–receptor bonds.

For the convenience of the readers, in section 2, we define the term ‘soft mechano-chemistry’ and explain the protocols of MFS that are normally followed in soft-mechanochemistry. Next, in section 3, we present a brief critical summary of our earlier works [3–6] on some of the molecular joints in a mitotic spindle, and propose new analysis of the corresponding results in terms of relevant time scales and length scales. Then, in section 4, we develop a new model for an important molecular hub formed by MTs in a spindle that, to our knowledge, has not been investigated in the past from the perspective of MFS. We report the results obtained by *in silico* MFS of this new model. We highlight the main features of the new results by comparing and contrasting with those of the corresponding results [3–6] for the other joints formed by MTs in a mitotic spindle. In section 5 we compare the trend of variation of the mean lifetime of the crosslinked antiparallel MTs with those of other molecular hubs in the spindle formed by tethering of MTs to their specific binding partners. We also compare these molecular hubs with other MT attachments in living cells to link our work with an even broader varieties of phenomena. Finally, in section 6 we conclude with a brief summary of the present status and plausible future direction of progress in soft mechano-chemistry of joints formed by MTs.

2. MFS in soft-mechanochemistry: a brief introduction

2.1. What is soft mechano-chemistry

Different areas of chemistry were classified by Nernst according to the type of input energy that induce the chemical changes; the familiar classes include, for example, electro-chemistry, photo-chemistry, thermo-chemistry, which are induced by electrical, optical, and thermal means, respectively [25]. Using the same terminology, mechano-chemistry is defined as the process of chemical activation by mechanical

force (or, more generally, mechanical stress). One unique feature of mechano-chemistry is that, utilizing the vector nature of force, the chemical kinetics can be altered drastically by merely changing the direction of the force without changing its magnitude. Making fire by rubbing pieces of wood against each other, which exploits mechanical stress for activating a chemical reaction, is one of the earliest experiences of mankind in mechano-chemistry. The earliest record of systematic study of mechano-chemistry can be traced back to those of Theophrastus of Eresus, a student of Aristotle, in the fourth century B.C. [26–28]. But, strangely, mechano-chemistry is not as widely known as, say, electro-chemistry.

In agreement with the IUPAC definition, throughout this paper, we use the term mechano-chemistry in its broadest sense, namely, the branch of chemistry where chemical reactions are induced by mechanical forces. We do not maintain any semantic distinction between mechano-chemistry and mechano-physics or that between mechano-chemistry and mechanical activation [29].

Most of the works on mechano-chemical phenomena till mid-twentieth century were restricted to covalent mechano-chemistry, where mechanical forces (usually in the range of nano-Newton) induce changes in a covalent bond (even its mechanical scission), and hence the name [30]. In contrast, rupture of mechanically resistant non-covalent bonds (e.g. hydrogen bonds), induced by weak forces (of the order of pico-Newton), can result in a conformational change of a macromolecule or detachment of two different macromolecules from each other. In this paper, we are exclusively interested in such non-covalent mechano-chemistry [31], also referred to as *soft* mechano-chemistry [32].

2.2. Protocols of MFS in vitro: slip- and catch bonds

In the 'force clamp' protocol of MFS a time-independent ('clamped') external tension F is applied on a pre-formed attachment. The time interval between the application of the external tension and the subsequent complete rupture of the attachment for the first time is defined as its lifetime $\tau(F)$ corresponding to the applied tension F. Similarly, in the 'force-ramp' protocol [17] the magnitude of the time-dependent external tension is gradually increased ('ramped up') following a well-defined prescription till the attachment ruptures completely. The value of the tension at which complete rupture of the attachment takes place for the first time is identified as the rupture force. The meaning of complete rupture is defined operationally for each system so that no ambiguity arises while interpreting the data. Because of the stochasticity of the rupture process, both the lifetime and rupture force fluctuate randomly from one sample to another of the same joint. From the probability distributions of the lifetimes, we compute the mean life time which is the main quantity of our interest in this paper.

For slip bonds, which are more common, the mean lifetime is a monotonically decreasing function of the externally applied tension. The distinct mechanical signature of a catch bond [33–37] is the non-monotonic variation of mean life time with the tension; at sufficiently weak tension the mean lifetime increases with increasing tension up to a maximum beyond which, like slip bonds, the lifetime decreases with further strengthening of the tension. The initial increase of lifetime with the magnitude of the clamped tension may appear counterintuitive because it implied stabilizing the joint, instead of the expected destabilization, with increasing magnitude of the tension. Since force-clamp provides the most direct evidence for catch bond, in this paper we present results obtained only under force-clamp conditions.

3. MFS of spindle HUBS: tethered microtubules

Each MT has a tubular structure. Each of these cylindrical tubes consists of 13 parallel protofilaments; each protofilament, in turn, is a linear sequence of tubulin dimers (α and β tubulin) of length 8 nm. In this section we review the results of both *in vitro* and *in silico* molecular force spectroscopic studies of the key molecular joints formed by MTs in a mitotic spindle.

3.1. MFS of microtubule–kinetochore attachment

Kinetochote (kt) is a macromolecular complex [38] located on the surface of the sister chromatids that result from DNA replication. In a correctly assembled mitotic spindle each kt remains attached to N MTs approaching it from each spindle pole; the numerical value of N of varies from one species of organism to another [15, 39]. In this subsection we review the quantitative results obtained so far from molecular force spectroscopic studies of kt–MT attachments *in vitro* and the corresponding theoretical models *in silico*.

3.1.1. Spindle of budding yeast: single MT per kinetochore. In budding yeast each kt can attach with only a single MT [40]. Using reconstituted kt–MT attachments of the budding yeast *in vitro*, nonmonotonic variation of the average lifetime with applied tension was observed in force-clamp experiments [41, 42]. Thus, over a range of small values of tension, the kt–MT attachment is further stabilized, rather than destabilized, by increase of the strength of the tension. This apparently counterintuitive trend of variation of the mean lifetime with external tension is very similar to that of ligand–receptor 'catch-bonds' [41]. Motivated by those experimental studies, Sharma *et al* [3] developed a minimal model (from now referred to as the SSC model) to provide an understanding of the physical origin of the catch-bond-like behaviour of the kt-MT attachments. After summarizing the main results and physical interpretations of reference [3], we analyze the same results here from a different perspective in terms of fundamental time scales and length scales in the problem.

The SSC model [3] implicitly assumes an effective 'sleeve-like' kt–MT coupler. The MT can be inserted into the sleeve coaxially because the outer diameter of the MT is slightly smaller than the inner diameter of the sleeve. The sleeve is oriented perpendicular to the kinetochore plate; the sleeve is connected to the kinetochore plate by rigid rod-like attachments (see figure 1(a)). The choice of this coupler is inspired by the 'sleeve model' of the kt–MT coupler postulated originally by Hill [43–46]. Subsequent discovery of the Dam1 ring [47] and the rod-like protein Ndc80 [48–50] provide justification of

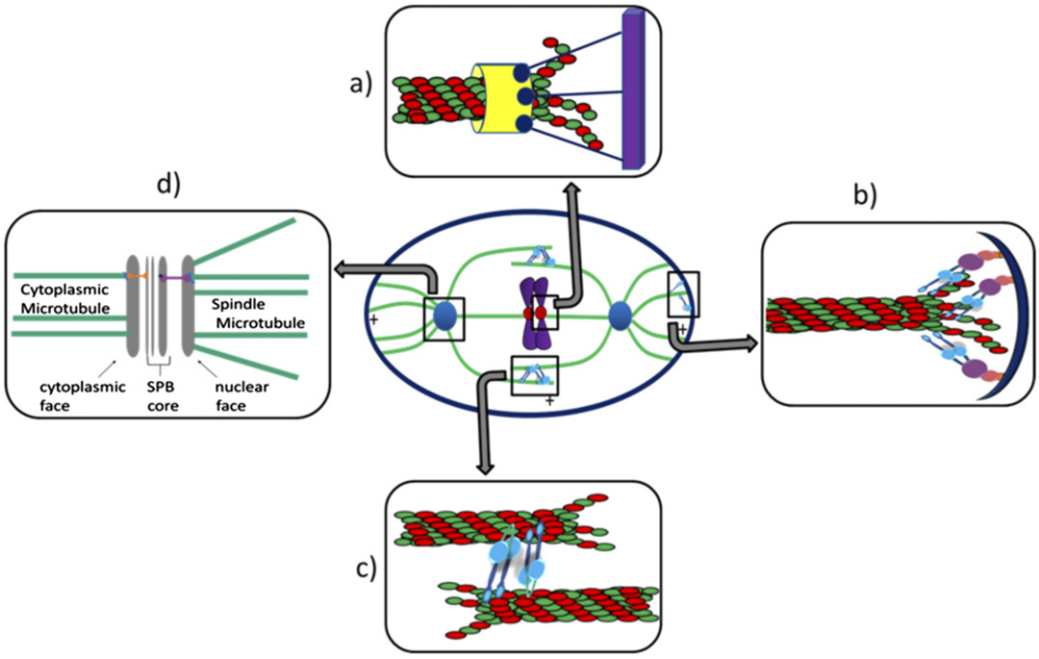

Figure 1. A cartoon of the mitotic spindle indicating the location of key molecular hubs where microtubules form transient molecular joints. (a) Kinetochore microtubules interact with kinetochores; the kinetochore–microtubule attachment is necessary for chromosome segregation. (b) Astral microtubules interact with cell cortex through dynein motors whose tail remains anchored on the cortex. (c) Interpolar microtubules nucleate from two opposite poles and their antiparallel plus ends are crosslinked by active molecules (molecular motors) as well as passive crossbridging molecules. (d) The minus ends of the microtubules remain anchored on the spindle pole bodies (centrosomes) throughout mitosis. Reproduced with permission from [6].

the sleeve-like coupler. Although the Hill model was extended later by incorporating further details [45, 46, 51] none of those detailed features were captured in the SSC model. Therefore, the simplest version of the SSC model described below may be regarded as a minimal model of the kt–MT attachment.

In the SSC model the overlap between the outer surface of the MT and the inner surface of the sleeve is denoted by a time-dependent continuous variable $y(t)$ $(0 \leqslant y(t) \leqslant L)$ where L is the total length of the sleeve. This model is based on the following two postulates [3]:

Postulate (I) The kt–MT interaction potential $V_b(y) = -By$, where B is the constant of proportionality, is quantification of the assumption that energy decreases linearly the increase of the overlap y; this potential is a special limit of the potential assumed in Hill's sleeve model [43].

Postulate (II) The depolymerization rate $\beta(F)$ of the MT decreases exponentially with increasing external tension F as given by

$$\beta(F) = \beta_0 \exp(-F/F_\star), \tag{1}$$

where β_0 is the tension-free rate of depolymerization and the parameter $F_\star$ characterizes the sharpness of the decrease of $\beta(F)$ with increasing F. *In vitro* experiment [52] has demonstrated decrease of $\beta(F)$ with increasing F. The time taken by the overlap $y(t)$ to vanish *for the first time* was defined as the life time of the attachment. Since the rupture of the kt–MT attachment is a stochastic process, the lifetime has a statistical distribution even if the initial overlap L_0 $(0 < L_0 \leqslant L)$ is a constant; the mean of this distribution can be compared with the corresponding mean lifetime τ obtained from experiments.

The stochastic kinetics of the kt–MT attachment in the SSC model can be mapped onto that of a hypothetical overdamped Brownian particle whose position in a one-dimensional space is given by the overlap variable $y(t)$ and it experiences an external potential $V(y) = -By + Fy$. Since we are interested in the arrival of the particle at $y = 0$ only for the first time, an *absorbing* boundary condition is imposed at $y = 0$ for the calculation of the life times. The *reflecting* boundary condition at $y = L$ captures the physical fact that the MT does not penetrate the kinetochore plate. Accordingly, the kinetics of this hypothetical Brownian particle can be formulated in terms of a Fokker–Planck (FP) equation [53, 54] with a reflecting boundary at $y = L$, an absorbing boundary at $y = 0$ and one of the initial conditions mentioned above.

In reference [3] the mean lifetime τ corresponding to the initial condition $y(t = 0) = L$ was found to be

$$\tau = \frac{D}{v^2(F)}\left[\mathrm{e}^{v(F)L/D} - 1\right] - \frac{L}{v(F)} \tag{2}$$

where D is the diffusion constant and the force-dependent drift velocity $v(F)$ of the hypothetical Brownian particle, given by

$$v(F) = \frac{B - F}{\Gamma} + (\alpha - \beta(F))\ell = \frac{B - F}{\Gamma} + (\alpha - \beta_0 \mathrm{e}^{-F/F_\star})\ell, \tag{3}$$

involves a phenomenological coefficient Γ, that characterizes the viscous drag on it, and ℓ denotes the increase of the length of the MT upon addition of a single subunit.

The external tension F has two opposite effects on the MT. It pulls the MT out of the coupler thereby tending to decrease the overlap $y(t)$. Simultaneously, it suppressed MT depolymerization without affecting its polymerization. rate Consequently, if the rate $\beta(F)$ of depolymerization falls below that of polymerization the tip of the MT exhibits a net growth which tends to increase the overlap $y(t)$. A catch-bond-like behavior would be exhibited if such an increase of $y(t)$ resulting from the polymerization-depolymerization kinetics of the MT can more than compensate the decrease of $y(t)$ caused by its bodily displacement in response to the pull. In contrast, if the tension-induced suppression of the depolymerization is so weak that the bodily movement of the MT out of the sleeve cannot be compensated by the growth of its tip into the sleeve, the kt–MT attachment would exhibit a slip-bond-like behavior.

Calculation of the mean lifetime of the model kt–MT attachment needs a well defined initial value of $y(t = 0)$ (denoted, for convenience, by L_0). In reference [3] L_0 was assumed to be equal to L for all samples over which the data obtained for the lifetime of the attachment were averaged. It is worth checking how the mean lifetime varies with the magnitude of L_0 [4]. Since it has not possible to measure L_0 for any kt–MT attachment used for MFS studies *in vitro*, an alternative, and more realistic, choice of the initial condition would be to select L_0 randomly, with uniform probability over the range $0 < y(t = 0) \leqslant L$; in this case computation of the mean lifetime required further averaging over the distribution of initial conditions [4].

The mean lifetime of the model kt–MT attachment corresponding to the fixed initial condition $L_0 = L$ [3] as well as those corresponding to the uniformly distributed random initial condition L_0 ($0 < L_0 \leqslant L$) [4] exhibit catch-bond-like behavior provided F_* is sufficiently small, i.e., if the depolymerization rate $\beta(F)$ decreases sufficiently sharply with increasing F. However, beyond a range of F_* the sharpness of the fall of $\beta(F)$ with F is not adequate to result in a catch-bond and, consequently, a slip-bond-like behavior would be observed (see figure 3 of [3]). Suppose, the peak in the τ versus F plot appears at $F_{\rm peak}$. The mean lifetime τ for a fixed F ($F > F_{\rm peak}$) increases exponentially with L_0 provided L_0 is not too small (see figure 3 of [4]).

3.1.2. A new analysis in terms of time- and length-scales. We now present a new analysis of the expression (2) in terms of the two fundamental time scales in the problem. If the Brownian particle had to traverse a distance of L purely diffusively, on the average, it would take a time

$$\tau_{\rm D} = \frac{1}{2}\frac{L^2}{D}. \tag{4}$$

On the other hand, if the same distance had to be covered ballistically with the velocity v, the time needed would be

$$\tau_{\rm B} = \frac{L}{v}. \tag{5}$$

The expression (2), recast as

$$\tau = \frac{1}{2}\frac{\tau_{\rm B}^2}{\tau_{\rm D}}[{\rm e}^{2\tau_{\rm D}/\tau_{\rm B}} - 1] - \tau_{\rm B} \tag{6}$$

shows transparently the interplay of diffusive time $\tau_{\rm D}$ and ballistic time $\tau_{\rm B}$. In the limit $\tau_{\rm D} \ll \tau_{\rm B}$, $\tau \simeq \tau_{\rm D}$, i.e., the kt–MT joint can get ruptured by pure diffusion.

Next, in order to interpret the observed L-dependence of τ, we introduce the fundamental length scale $\Lambda = 2(D/v)$. In terms of Λ, the mean lifetime in diffusive limit can also be expressed as

$$\tau \simeq \frac{1}{2}\frac{L^2}{D} \quad \text{for } L \ll \Lambda. \tag{7}$$

In the opposite limit, from (2), we get

$$\tau \simeq \frac{1}{2}\frac{\Lambda}{v}\,{\rm e}^{L/\Lambda} \quad \text{for } L \gg \Lambda. \tag{8}$$

3.1.3. Spindle of mammalian cells: multiple MTs per kinetochore. The SSC model was generalized and re-interpreted appropriately [4] to capture the key features of the energetics and kinetics for kt–MT attachments in higher eukaryotic organisms for which $N > 1$. In order to avoid any confusion, this attachment will be referred to as kt–NMT attachment. By construction, initially all the N MTs are attached to a single kt. But, at any subsequent time before complete rupture, the actual number of MTs still attached to the same kt is $n(t) \leqslant N$; complete rupture of the attachment corresponds to $n = 0$. The time t at which $n(t)$ vanishes for the first time is defined as the lifetime of the attachment.

Two features of this system, which were absent in the case of budding yeast (i.e., $N = 1$) are the following:

(a) When a MT detaches from the kt, its load is instantaneously redistributed among the $n(t)$ MTs that are still attached to the kt at that instant of time thereby affecting the likelihood of detachment of the surviving MTs and, in turn, the overall stability of the attachment; and

(b) A detached MT can re-attach, as long as $n(t) \geqslant 1$, thereby prolonging the overall life of the kt–NMT attachment.

The mean life time data, reported originally in reference [4], are replotted against the clamp force in figure 2(a) for a fixed value of N ($N = 40$). Interestingly, the catch-bond-like behavior is displayed irrespective of whether rebinding of the MTs is allowed or not. Nevertheless, as expected, for any given tension F, the mean life time τ is higher if rebinding is allowed as compared to that in the absence of rebinding. The physical origin of the catch-bond-like behavior for all $N > 1$ is, however, identical to that in the special case $N = 1$.

The mean lifetime is increases sub-linearly with the number of microtubule (N), as shown in figure 2(b). The lifetime of the attachment is an emergent property of the system consisting of a single kt interacting with a bundle of N parallel MTs. It is worth emphasizing that the parallel MTs do not interact laterally with one another; the indirect interaction between the MTs arises from the load sharing. The N-dependence of τ can, in principle, be tested in near future with the mammalian kt reconstituted *in vitro* [55, 56].

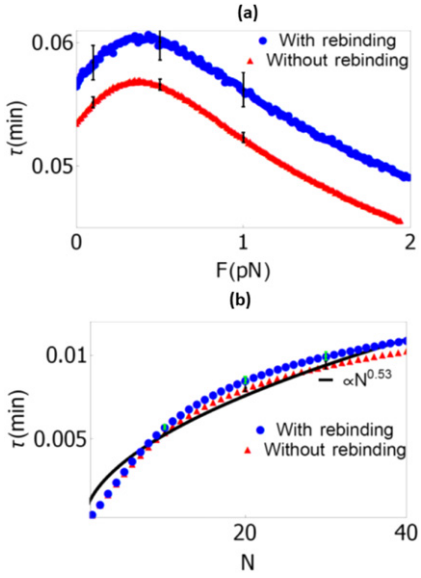

Figure 2. The mean lifetime τ of a kt–NMT coupler, reported originally in reference [4], is replotted against (a) F for $N = 40$ and (b) N for $F = 10$ pN, both with (blue circle) and without (red triangle) rebinding. The error bars for the simulation data are also shown explicitly in (a). For the numerical values of the remaining parameters used for this plot, see reference [4]. The best fit to our simulation data, given by $\tau \propto N^{0.53}$, is represented by the black continuous line in (b). Reprinted figure with permission from [4], ©2018 the American Physical Society.

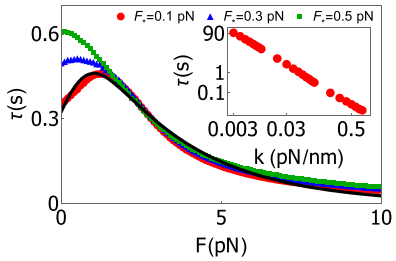

Figure 3. Mean lifetime τ of the MT–ct attachment is plotted against the applied external tension F for three different values of $F_\star$, namely $F_\star = 0.1, 0.3, 0.5$ pN, at fixed $N_\mathrm{d} = 10$, where N_d is the maximum number of dynein motors that can simultaneously tether the MT to the cortex. The solid black line is the best fit to the data for $F_\star = 0.1$ pN, log–log plot of the mean lifetime τ as a function of spring stiffness k, for fixed $F = 0.1$ pN, is shown in the inset. See reference [5] for the numerical values of all the other parameters used in the simulation. Reprinted figure with permission from [5], ©2018 the American Physical Society.

3.2. MFS of a microtubule–cortex attachment

The interactions of astral MTs with the cell cortex are major determinants of the position and orientation of the spindle [57]. In reference [5], we have developed a minimal theoretical model of a single MT tethered to the cell cortex by dynein motors. The tails of the dyneins are assumed to be permanently anchored on the cell cortex while their heads tend to walk along the minus ends of the MT. In contrast to the passive linkers that couple the kt with the MT, the dynein motors are active protein; they use a chemical fuel (ATP) for their mechanical function. The unbinding of the heads of these cyclic motors from the MT during each of their respective cycles can hasten the rupture of the attachment unless its rebinding or fresh binding of other motors occur sufficiently rapidly.

We have computed the lifetime of this model attachment by implementing the same protocols of MFS *in silico* that we used earlier for the kt–MT attachment [5]. The mean lifetime of the model ct–MT attachment is plotted in figure 3 for three different values of the characteristic force $F_\star$. For $F_\star = 0.1$ pN, the mean lifetimes (plotted with red circles) exhibit catch-bond-like non-monotonic variation with the external tension F. With the increase of $F_\star$ (see the data for $F_\star = 0.3, 0.5$ pN in figure 3), the nature of the ct–MT attachment crosses over to a typical slip bond.

4. MFS of spindle HUBS: crosslinked antiparallel MTs

In the metaphase spindle the interpolar MTs, originating from two opposite poles of the spindle, get crosslinked in the equatorial plane by crosslinking molecules [12]. Active crosslinkers generate pushing or pulling forces by hydrolyzing ATP and exert those forces on the antiparallel MTs [58]. The common active cross-linkers are cytoskeletal motors, like kinesin-5. Kuan and Betterton [59] investigated the accumulation of the motors on crosslinked antiparallel MTs by developing a model that is an appropriate extension of the totally asymmetric simple exclusion process [60]. The *in vitro* experiment performed by Shimamoto *et al* [61] and their numerical simulation of a model developed to capture the key features of this experiment is closest to our theoretical work reported here. We have studied the strength and stability of a pair of antiparallel interpolar MTs *in silico*, crosslinked by active crosslinkers, by applying external force on the attachment.

4.1. Model of two crosslinked antiparallel MTs

For simplicity, our theoretical model considers only two colinear MTs that are oriented antiparallel with respect to each other (see figure 4(a)). The lower MT is immobilized on a fixed horizontal plane; so, no bodily movement of this lower MT is possible. We place the origin of the coordinate system on the negative end of the lower MT (its left edge in figure 4(b)) which is assumed to be rigidly attached to a vertical surface. We apply an external force F on the minus end of the top MT. This set up in our *in silico* experiment is very similar to that used by Shimamoto *et al* [61] for their experiment *in vitro*.

We represent a MT by a one-dimensional discrete lattice with lattice constant 8 nm. None of the sites on the top and bottom MT can be occupied by more than one crosslinker. Each active crosslinker (motor) has four heads, one pair of which walks, in a hand-over-hand stepping pattern, along the top MT while the other pair walks similarly along the bottom MT. For simplicity, we replace each of this pairs of motor heads by the corresponding mid-point and denote the position of the ith midpoint by the symbols $x_i^{\mathrm{T,B}}$ where the superscripts T and B refer to the top and bottom MT, respectively, with which the ith midpoint is associated. From now onwards, for the economy of words, we refer to the midpoints themselves as motor heads. We model the linkage between the two heads of each

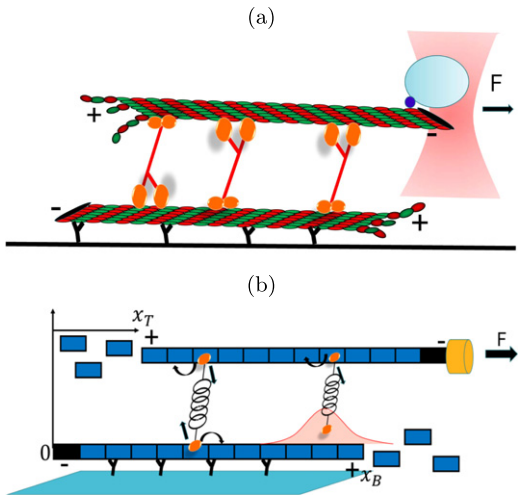

Figure 4. (a) A schematic depiction of the pair of antiparallel MTs crosslinked non-covalently using active crosslinking molecules (four-headed molecular motors) in a hypothetical *in vitro* experiment. Bottom MT is immobilized on a glass plate and external force F is applied on the top MT. Polymerization and depolymerization are allowed only at the plus-end of each MT. The active crosslinkers (orange) walk directionally only towards the plus-ends of the MTs. (b) A description of our theoretical model for the experimental set up depicted in (a). Origin coincides with the minus-end of the bottom MT; x_B and x_T represent, respectively, the distance of the plus-ends of the bottom and top MTs from the origin. Of the four-heads of each active crosslinker the pair that walks along the same MT is replaced by the corresponding mid-point. Horizontal arrows on the heads indicate the allowed direction of hopping on the lattice. Boltzmann distribution for the position of the single unbound head of a crosslinker at room temperature is shown by the shaded area around a site where it can attach ($k = 1$ pN nm^{-1}).

crosslinker by an elastic Hookean spring of stiffness k. In our model each a midpoint, representing a pair of heads of an active motor, is allowed to walk towards only the plus-end of the respective MT track using ATP as fuel.

Let N denote the maximum total number of crosslinkers that can simultaneously bind to at least one of two antiparallel MTs whereas $n(t)$ denotes the corresponding actual number at any arbitrary instant of time t (i.e., $n(t) \leqslant N$). For any given crosslinker, none of whose two heads are bound to the MTs, $\mathcal{K}_{\rm on}$ denotes the rate of binding of one of its heads to either of the two MTs. Therefore, at any arbitrary instant of time t, the rate of the event of binding of the first head of any of such unbound crosslinkers to either of the two MTs is [62]

$$k_{\rm on}(n) = \Big(N - n(t)\Big)\,\mathcal{K}_{\rm on}. \tag{9}$$

For a crosslinker that has only one of the two heads already bound to one of the MTs the remaining unbound head can bind to an empty site on the opposite MT with the binding rate $\mathcal{K}_{\rm on}$ thereby crosslinking the two MTs.

The externally applied force F pulls the top MT away from the origin thereby stretching the Hookean springs. So, the restoring force acting on a crosslinking molecule (i.e., a crosslinker whose two heads are bound to the two distinct MTs) is

$$f_i = k(x_i^{\rm T} - x_i^{\rm B}). \tag{10}$$

Therefore, even if the heads of a MT crosslinking two MTs remain bound to two fixed sites on the two MTs and step neither forward nor backward on the respective MTs, the spring force acting on it can change, because of the change of spring length, as the top MT moves in response to the externally applied force F on it. Moreover, whenever any head of crosslinker bound to two MTs steps towards the plus-end or minus-end, the spring gets stretched and the spring force acting on it changes accordingly.

If only one of the two heads of an active crosslinker is bound to a MT, then it can hop only towards the plus-end of the MT with rate $k_{\rm hop}(0)$. But, if its both heads are bound to the two MTs crosslinking them then a head of the motor can hop forward with the load-dependent rate

$$k_{\rm hop}(f_i) = k_{\rm hop}(0)\mathrm{e}^{f_i/F_{\rm hop}} \tag{11}$$

with characteristic force $F_{\rm hop}$ which can be expressed as $k_{\rm B}T/\ell$ where ℓ is the length of a single subunit of MT.

Let $k_{\rm off}(0)$ denote the rate of unbinding of a single head of a crosslinker that is bound to a MT. According to the Bell–Kramers theory [63, 64] he effective rate of unbinding of any head of a crosslinker whose both heads are attached to the two MTs is approximately

$$k_{\rm off}(f_i) = k_{\rm off}(0)\mathrm{e}^{|f_i|/F_{\rm d}}. \tag{12}$$

The characteristic 'detachment force' $F_{\rm d}$ can be expressed as $F_{\rm d} = k_{\rm B}T/x_{\rm d}$ where $x_{\rm d}$ is the distance between the bound and unbound states of a crosslinker head.

The plus end of the bottom (B) and top (T) MTs are placed at distances $x_{\rm B}(t)$ and $x_{\rm T}(t)$, respectively, from the origin. The rates of polymerization and de-polymerization of the plus-end of a MT are given by α and β, respectively. The equation of motion of the top MT is given by

$$\frac{{\rm d}xT(t)}{{\rm d}t} = \frac{F - f_{\rm tot}}{\Gamma} + (\beta - \alpha)\ell + \frac{\eta(t)}{\Gamma} \tag{13}$$

where Γ in (13) is the effective viscous drag coefficient, $\eta(t)$ is a Gaussian white noise and ℓ, the length of each subunit of MT is also the step size of crosslinkers. In (13) the total force $f_{\rm tot}$ exerted on the top MT by all those crosslinking molecules whose two heads are bound to two MTs is

$$f_{\rm tot} = \sum_i f_i \tag{14}$$

where f_i is given by (10).

Note that vanishing of the overlap between the two MTs does not necessarily imply rupture of the attachment because even in that condition the two MTs may remain crosslinked by stretched springs. Therefore, we define the instant of rupture

Table 1. Numerical values of the parameters used in simulation.

Parameter	Values
Rate of binding of active crosslinker to MT $\mathcal{K}_{on}$ [68]	0.316 s^{-1}
Rate of unbinding of active crosslinker from MT $k_{off}(0)$ [66, 68, 92, 93]	1.56 s^{-1}
Rate of forward stepping of active crosslinker $k_{hop}(0)$	100 s^{-1}
Characteristic detachment force F_d	50 pN
Characteristic hopping force of active crosslinker F_{hop}	10 pN
Spacing between binding sites on MT ℓ	8 nm
Rate of polymerization of MT α	0 s^{-1}
Rate of depolymerization of MT β_0	0 s^{-1}
Spring constant k	1 pN nm^{-1}
Effective drag coefficient Γ	60 pN s μm^{-1}

of the attachment as the time when for the *first time* none of the crosslinkers has both heads attached to the two MTs and, simultaneously, there is no overlap between top and bottom MTs. This '*first passage time*' is identified as the lifetime of the attachment.

4.2. Simulation method and results

We have carried out Monte Carlo simulation of our model. The lengths of both the top and bottom MTs have been chosen to be 800 nm. The common parameter values used in the simulation are listed in table 1. We have assumed truncated Gaussian distribution for the spring of the single head bounded crosslinkers. For a crosslinker whose one head is attached to one of the MTs, the other (unbound) head can only crosslink to opposite MT following the truncated Gaussian distribution (shaded area in figure 4(b)). A suitable location for binding of the free head of the crosslinkers is calculated by taking inverse transform sampling of the distribution for each iteration.

In the initial configuration both of the MTs overlap each other entirely. Moreover, initially both heads of each of the crosslinkers were bound to the opposite sites located on the two MTs. With this initial condition at time $t = 0$, we applied external force on the top MT. Then in each time step Δt crosslinkers can bind/unbind and hop forward/backward on the MTs according to the rates specified above. During the same period Δt, the MTs can also polymerize/depolymerize or move bodily in the forward/backward direction depending upon the direction of the external force. The time evolution of this system is monitored until the attachment ruptures (see the definition of rupture in the preceding subsection). After averaging over sufficiently large number of samples, we get the mean lifetime of the attachment.

In figure 5 we plot mean lifetime of the crosslinked antiparallel MT attachment as a function of the external force F. In order to emphasize the role of the crosslinker motors on the stability of the attachment, we have plotted τ/τ_{max} where τ_{max} is the highest lifetime for a given value of N. The mean lifetime decreases monotonically with increasing magnitude of F which is a signature of slip-bond like behavior. The active crosslinkers slide the two mutually antiparallel MTs away from each other thereby reducing the extent of their overlap. Because of this tendency, the active crosslinkers have a tendency to destabilize these cross-linked attachments that manifests as a slip-bond.

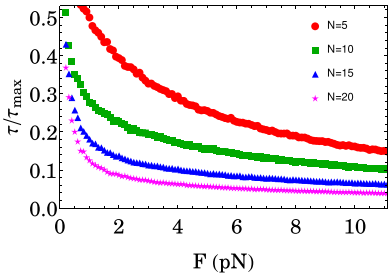

Figure 5. Mean lifetime of the anti-parallel MT attachment in the presence of active crosslinkers is scaled to one by dividing maximum lifetime i.e. the lifetime at $F = 0$ pN and plotting against external load F, for $N = 5$ (red circle) with $\tau_{max} = 17.74$ s, $N = 10$ (green square) with $\tau_{max} = 20.35$, $N = 15$ (blue triangle) with $\tau_{max} = 28.85$ and $N = 20$ (pink star) with $\tau_{max} = 42.29$ s. All the points are obtained from computer simulation and corresponding parameters are given in table 1.

5. Comparison of various attachments formed by MT

The plus ends of the kinetochore MTs are *tethered* to the kinetochores (see figure 1(a)) while that of the astral MTs are *tethered* to the cell cortex by the respective molecular tethers (see figure 1(b)). In contrast, the plus ends of the ipMTs are *crosslinked* at the equatorial plane of the spindle (see figure 1(c)). Over the last five years we have studied the strength and stability of all the three types of attachments. In our earlier publications [4, 5] we reported the results of *in silico* MFS of MT–kt and MT–cortex attachments. In this paper we have reported, for the first time, the results for two antiparallel ipMTs crosslinked by active crosslinkers.

The crosslinked antiparallel interpolar MTs play a crucial role in maintaining the structural integrity and stability of the spindle [65]. As our results establish here, the active crosslinkers tend to destabilize such attachments. In sharp contrast, passive crosslinkers can increase the overlap between the two crosslinked antiparallel MTs by sliding these with respect to each other with forces that are of entropic origin [66, 67]. Ase1-GFP is a well studied example of passive crosslinkers. Johann *et al* [68] and Guha *et al* [69] developed minimal models to study the competition between active

and passive crosslinkers. Moreover, the passive crosslinkers generate effective friction between the two antiparallel MTs; the microscopic origin of this friction has been elucidated by Wierenga and Rein ten Wolde [70]. Work on *in silico* MFS of antiparallel MTs crosslinked by a mixture of active and passive crosslinkers is in progress [71].

The molecular biomechanics of the negative ends of all the three types of MTs, which are *anchored* on macromolecular complexes located at the spindle poles (see figure 1(d)), has just begun to receive attention from the perspective of MFS. Fong *et al* [72] purified spindle pole bodies (SPB) from budding yeast. Preparing an attachment of a single MT with the SPB *in vitro*, they tested its strength using the force-ramp protocols of MFS. The mean rupture force of this attachment turned out to be approximately four times higher than that of the kt–MT attachment under identical loading conditions. Fong *et al* [72] speculated that the higher rupture force of the SPB–MT is essential for maintaining the structural integrity of the spindle. The relative magnitudes of the two attachments ensures that the MT remains firmly anchored on the SPB and the laminar structure of the SPB remains intact even when the kt–MT attachment gets ruptured. Work on the development of a theoretical model for this pole–MT attachment and its MFS *in silico* is now in progress; the results will be reported elsewhere in future [73].

In this paper we have assumed both the MTs to be perfectly rigid and the external tension has been applied in a direction colinear with the MTs. In case of MTs much longer than their persistence length, the filament can be approximated by a semi-flexible polymer; in that case, it would be interesting to explore the consequence of applying the force in a direction making an angle with the attached linear segment. In the commonly used geometry of gliding assay, MTs float on a flat surface onto which the tails of two-headed motors are anchored while the heads tends to walk on the MTs thereby causing gliding of the MT on the surface. The protocol used for studying force-induced desorption of a semi-flexible MT crosslinked with a surface by motors, a situation that mimics gliding assay, is similar to force-ramp protocol of MFS [74].

Mitotic spindle is not the only filamentous network formed by MTs in eukaryotic cells. Distinct types of MT network architectures emerge in different types of cells and even during different phases of the cell cycle of a single cell [75–80]. It would be interesting to probe molecular hubs in those MT networks from the perspective soft mechano-chemistry using MFS.

6. Conclusion: past, present and prospects of soft mechano-chemistry

In the words of Karplus [81], 'the ligand can be as small as an electron, an atom or diatomic molecule and as large as a protein'. This definition of a ligand has been extended even further in our works on the various molecular hubs of mitotic spindle depicted in figure 1 where we treat a MT [16] as a 'ligand' and its binding partner as a 'receptor'. The conditions implemented in our simulations of the various MT–receptor models are essentially *in silico* analogs of the 'force-clamp' and 'force ramp' protocols of *in vitro* MFS carried out with common chemical ligand–receptor bonds [82].

Biomechanics is a sub-discipline of mechanics (as well as that of biophysics, and biomedical engineering). *Molecular biomechanics* focuses mainly on the mechanical aspects of biomolecules, which includes, for example, force-induced structural (or conformational) changes and unfolding of biomolecules and even rupture of non-covalent inter-molecular bonds. Therefore, the results of our *in silico* molecular force spectroscopic studies of the various attachments formed by MTs are contributions to molecular biomechanics. In contrast, *mechano-biology* is a sub-discipline of biology. *Molecular mechano-biology* is mainly concerned with control and regulation of the biological functions of biomolecules by mechanical stress and functional response of biomolecules to mechanical stress.

It is worth asking the implications of the results of our studies in molecular biomechanics in molecular mechano-biology. Catch bond is known to facilitate mechano-sensing [83–85]. Important roles of mechanical forces in the stabilization of proper chromosome configuration in a mitotic spindle have been known for a long time [86, 87]. More specifically, in the context of our studies, what may be the biological functional advantages of a catch-bond over a slip-bond? An answer to this question may provide a clue as to why some of the attachments formed by MTs in a spindle are catch-bonds whereas the others are just slip-bonds. In recent times a catch-bond-based mechanism of '*mechanical proofreading*' has received serious attention in the literature. It is one of the three possible mechanisms of mechanical proofreading that have been proposed [88]. Increased bond lifetime with increasing tension, as happens in the case catch-bonds, may enable a receptor to select for the specific ligands which form catch bond with it.

From our investigations so far, it appears that there is a significant qualitative difference between the MT–kt, MT–ct attachments on one hand, and the crosslinked ipMTs on the other. Over a physiologically relevant parameter range the former exhibits catch-bond like behavior whereas the latter always remains a slip bond. These behaviors might have been shaped by evolution. In the light of mechanical proofreading, our results would imply that attachments (crosslinks) formed by the antiparallel ipMTs do not involve the kind of specificity that is involved, for example, in the formation of the MT–kt attachment. This particular implication needs a thorough investigation in future.

The term '*emergent mechanics*' has been coined [89] for conceptual framework needed to account for the emergent collective spatial and temporal patterns of such multi-component scaffolds in terms of the chemo-mechanical interactions and dynamics of their building blocks. Our studies of the soft chemo-mechanics of the key molecular joints in the spindle is likely to provide insights into the mechanisms of integration of operation of these joints [90] in the overall emergent mechanics of the mitotic spindle [91].

Acknowledgments

We thank Ajeet K Sharma, Blerta Stylla, Subhadeep Patra and Raymond Friddle for enjoyable collaborations reported earlier in references [3–5] some of which have been reviewed briefly in this paper. Research work of one of the authors (DC) has been supported by SERB (India) through a J C Bose National Fellowship.

ORCID iDs

Debashish Chowdhury https://orcid.org/0000-0002-0536-2321

References

[1] Nagel S R 2017 Experimental soft matter science *Rev. Mod. Phys.* **89** 025002
[2] Jones R A L 2004 *Soft Condensed Matter* (Oxford: Oxford University Press)
[3] Sharma A K, Shtylla B and Chowdhury D 2014 Distribution of lifetimes of kinetochore-microtubule attachments: interplay of energy landscape, molecular motors and microtubule (de-)polymerization *Phys. Biol.* **11** 1478
[4] Ghanti D, Patra S and Chowdhury D 2018 Molecular force spectroscopy of kinetochore-microtubule attachment in silico: mechanical signatures of an unusual catch bond and collective effects *Phys. Rev.* E **97** 052414
[5] Ghanti D, Friddle R W and Chowdhury D 2018 Strength and stability of active ligand-receptor bonds: a microtubule attached to a wall by molecular motor tethers *Phys. Rev.* E **98** 042415
[6] Ghanti D 2018 Stochastic kinetics of transient joints in multicomponent molecular machines: fluctuating force, collective behaviour and emergent chemo-mechanics *PhD Thesis* IIT Kanpur
[7] Chowdhury D 2013 Stochastic mechano-chemical kinetics of molecular motors: a multidisciplinary enterprise from a physicist's perspective *Phys. Rep* **529** 1–197
[8] Kolomeisky A B 2015 *Motor Proteins and Molecular Motors* (Boca Raton, FL: CRC Press)
[9] Zheng Y *et al* 2010 An integrated overview of spationtemporal organization and regulation in mitosis in terms of the proteins in the functional supercomplexes *Front. Microbiol.* **5** 573
[10] Karsenti E and Vernos I 2001 The mitotic spindle: a self-made machine *Science* **294** 543–7
[11] Bouck D C, Joglekar A P and Bloom K S 2008 Design features of a mitotic spindle: balancing tension and compression at a single microtubule kinetochore interface in budding yeast *Annu Rev. Genet.* **42** 335–59
[12] McIntosh J R, Molodotson M I and Ataullakhanov F I 2012 Biophysics of mitosis *Q. Rev. Biophys.* **45** 147–207
[13] McIntosh J R and Hays T 2016 A brief history of research on mitotic mechanisms *Biology* **5** 55
[14] Mogilner A and Craig E 2010 Towards a quantitative understanding of mitotic spindle assembly and mechanics *J. Cell Sci.* **123** 3435–45
[15] Petry S 2016 Mechanisms of mitotic spindle assembly *Annu. Rev. Biochem.* **85** 659
[16] Lawson J L D and Salas R E C 2013 Microtubules: greater than the sum of the parts *Biochem. Soc. Trans.* **41** 1736
[17] Bowne-Anderson H, Zanic M, Kauer M and Howard J 2013 Microtubule dynamic instability: a new model with coupled GTP hydrolysis and multistep catastrophe *BioEssays* **35** 452
[18] Sutradhar S, Yadav V, Sridhar S, Sreekumar L, Bhattacharyya D, Ghosh S K, Paul R and Sanyal K 2015 A comprehensive model to predict mitotic division in budding yeats *Mol. Biol. Cell* **26** 3954–65
[19] Gralka M and Kroy K 2015 Inelastic mechanics: a unifying principle in biomechanics *Biochim. Biophys. Acta, Mol. Cell Res.* **1853** 3025–37
[20] Evans E 2001 Probing the relation between force-lifetime-and chemistry in single molecular bonds *Annu. Rev. Biophys. Biomol. Struct.* **30** 105
[21] Evans E and Williams P 2002 *Physics Of Biomolecules and Cells* ed H Flyvbjerg, F Jülicher, F Ormos and F David (Berlin: Springer)
[22] Friddle R W 2012 *Dynamic Force Spectroscopy and Biomolecular Recognition* ed A R Bizzarri and S Cannistraro (Boca Raton, FL: CRC Press)
[23] Arya G 2016 Models for recovering the energy landscape of conformational transitions from single-molecule pulling experiments *Mol. Simul.* **42** 1102–15
[24] Dudko O K 2016 Decoding the mechanical fingerprints of biomolecules *Q. Rev. Biophys.* **49** 1–14
[25] Fernandez-Bertran J F 1999 Mechanochemistry: an overview *Pure Appl. Chem.* **71** 581–6
[26] Takacs L 2013 The historical development of mechanochemistry *Chem. Soc. Rev.* **42** 7649–59
[27] Boldyrev V V and Tkacova K 2000 Mechanochemistry of solids: past, present, and prospects *J. Mater. Synth. Process.* **8** 121–32
[28] Beyer M K and Clausen-Schaumann H 2005 Mechanochemistry: the mechanical activation of covalent bonds *Chem. Rev.* **105** 2921–48
[29] Kaupp G 2009 Mechanochemistry: the varied applications of mechanical bond-breaking *CrystEngComm* **11** 388–403
[30] Garcia-Manyes S and Beedle A E M 2017 Steering chemical reactions with force *Nat. Rev. Chem.* **1** 0083
[31] Makarov D E 2016 Mechanochemistry of biological and synthetic molecules *J. Chem. Phys.* **144** 030901
[32] Lavalle P, Boulmedais F, Schaaf P and Jierry L 2016 Soft-mechanochemistry: mechanochemistry inspired by nature *Langmuir* **32** 7265–76
[33] Thomas W E 2008 Catch bonds in adhesion *Annu. Rev. Biomed. Eng.* **10** 39
[34] Thomas W E, Vogel V and Sokurenko E 2008 Biophysics of catch bonds *Annu. Rev. Biophys.* **37** 399
[35] Sokurenko E V, Vogel V and Thomas W E 2008 Catch-bond mechanism of force-enhanced adhesion: counterintuitive, elusive, but … widespread *Cell Host Microbe* **4** 314
[36] Prezhdo O V and Pereverzev Y V 2009 Theoretical aspects of the biological catch bond *Acc. Chem. Res.* **42** 693
[37] Chakrabarti S, Hinczewski M and Thirumalai D 2017 Phenomenological and microscopic theories for catch bonds *J. Struct. Biol.* **197** 50–6
[38] Cheeseman I M 2014 The kinetochore *Cold Spring Harbor Perspect. Biol.* **6** a015826
[39] Pavin N and Tolic I M 2016 Self-organization and forces in the mitotic spindle *Annu. Rev. Biophys.* **45** 279–98
[40] Biggins S 2013 The composition, functions, and regulation of the budding yeast kinetochore *Genetics* **194** 817
[41] Akiyoshi B, Sarangapani K K, Powers A F, Nelson C R, Reichow S L, Arellano-Santoyo H, Gonen T, Ranish J A, Asbury C L and Biggins S 2010 Tension directly stabilizes reconstituted kinetochore-microtubule attachments *Nature* **468** 576
[42] Akiyoshi B and Biggins S 2012 Reconstituting the kintochore-microtubule interface: what, why, and how *Chromosoma* **121** 235
[43] Hill T 1985 Theoretical problems related to the attachment of microtubules to kinetochores *Proc. Natl Acad. Sci. USA* **82** 4404

[44] Joglekar A P and Hunt A J 2002 A simple, mechanistic model for directional instability during mitotic chromosome movements *Biophys. J.* **83** 42
[45] Asbury C L, Tien J F and Davis T N 2011 Kinetochores' gripping feat: conformational wave or biased diffusion? *Trends Cell Biol.* **21** 38
[46] Grishchuk E L 2017 *Centromeres and Kinetochores* ed B E Black (Berlin: Springer)
[47] Buttrick G J and Millar J B A 2011 Ringing the cahnges: energing roles for DASH at the kinetochore-microtubule interface *Chromosome Res.* **19** 393
[48] Westermann S, Drubin D G and Barnes G 2007 Structures and functions of yeast kinetochore complexes *Annu. Rev. Biochem.* **76** 563
[49] Davis T N and Wordeman L 2007 Rings, bracelets, sleeves, and chevrons: new structures of kinetochore proteins *Trends Cell Biol.* **17** 377
[50] Foley E A and Kapoor T M 2013 Microtubule attachment and spindle assembly checkpoint signalling at the kinetochore *Nat. Rev. Mol. Cell Biol.* **14** 25
[51] Efremov A, Grishchuk E L, McIntosh J R and Ataullakhanov F I 2007 In search of an optimal ring to couple microtubule depolymerization to processive chromosome motion *Proc. Natl Acad. Sci.* **104** 19017
[52] Franck A D, Powers A F, Gestaut D R, Gonen T, Davis T N and Asbury C L 2007 Tension applied through the Dam1 complex promotes microtubule elongation providing a direct mechanism for length control in mitosis *Nat. Cell Biol.* **9** 832
[53] Risken H 1996 *The Fokker–Planck Equation* (Berlin: Springer)
[54] Mirny L A and Needleman D J 2010 Quantitative characterization of filament dynamics by single-molecule lifetime measurements *Methods Cell. Biol.* **95** 583
[55] McIntosh J R, O'Toole E, Zhudenkov K, Morphew M, Schwartz C, Ataullakhanov F I and Grishchuk E L 2013 Conserved and divergemtn features of kinetochores and spindle microtubule ends from five species *J. Cell Biol.* **200** 459
[56] Weir J R *et al* 2016 Insights from biochemical reconstitution into the architecture of human kinetochores *Nature* **537** 249
[57] Wu H Y, Nazockdast E, Shelley M J and Needleman D J 2016 Forces positioning the Bmitotic spindle: theories, and now experiments *BioEssays* **38** 1600212
[58] Mann B J and Wadsworth P 2019 Kinesin-5 regulation and funtion in mitosis *Trends Cell Biol.* **29** 66–79
[59] Kuan H S and Betterton M D 2016 Motor protein accumulation on antiparallel microtubule overlaps *Biophys. J.* **110** 2034–43
[60] Schütz G M 2001 *Phase Transitions and Critical Phenomena* ed C Domb and J L Lebowitz (New York: Academic)
[61] Shimamoto Y, Forth S and Kapoor T M 2015 Measuring pushing and braking forces generated by ensemblesof kinesin-5 crosslinking two microtubules *Dev. Cell* **34** 669–81
[62] Muller M, Klumpp S and Lipowsky R 2008 Tug-of-war as a copperative mechanism for bidirectional cargo transport by molecular motors *Proc. Natl Acad. Sci.* **105** 4609
[63] Bell G I 1978 Models for the specific adhesion of cells to cells *Science* **200** 618
[64] Kramers H A 1940 Brownian motion in a field of force and the diffusion model of chemical reactions *Physica* **7** 284
[65] Forth S and Kapoor T M 2017 The mechanics of microtubule networks in cell division *J. Cell Biol.* **216** 1525–31
[66] Braun M, Lansky Z, Fink G, Ruhnow F, Diez S and Janson M E 2011 Adaptive braking by Ase1 prevents overlapping microtubules from sliding completely apart *Nat. Cell Biol.* **13** 1259
[67] Braun M, Lansky Z, Hilitski F, Dogic Z and Diez S 2016 Entropic forces drive contraction of cytoskeletal networks *BioEssays* **38** 474–81
[68] Johann D, Goswami D and Kruse K 2015 Generation of stable overlaps between antiparallel filaments *Phys. Rev. Lett.* **115** 118103
[69] Guha S, Ghosh S, Pagonabarraga I and Muhuri S 2018 Stabilization of overlapping biofilms by passive crosslinkers (arXiv:1808.09383)
[70] Wierenga H and Rein ten Wolde P 2019 Diffusible crosslinkers cause superexponential friction forces (arXiv:1906.02527)
[71] Chowdhury D *et al* 2020 in preparation
[72] Fong K K, Sarangapani K K, Yusko E C, Riffle M, Llauro A, Davis T N and Asbury C L 2017 Direct measurement of the strength of microtubule attachment to yeast centrosomes *Mol. Biol. Cell* **28** 1853
[73] Chowdhury D *et al* 2020 in preparation
[74] Chaudhuri A and Chaudhuri D 2016 Forced desorption of semiflexible polymers adsorbed and driven by molecular motors *Soft Matter* **12** 2157
[75] Subramanian R and Kapoor T M 2012 Building complexity: insights into self-organized assembly of microtubule-based architectures *Dev. Cell* **23** 874
[76] Dogterom M and Surrey T 2013 Microtubule organization *in vitro Curr. Opin. Cell Biol.* **25** 23
[77] Mimori-Kiyosue Y 2011 Shaping microtubules into diverse patterns: molecular connections for setting up both ends *Cytoskeleton* **68** 603
[78] Alfaro-Aco R and Petry S 2015 Building the microtubule cytoskeleton piece by piece *J. Biol. Chem.* **290** 17154
[79] Bartolini F and Gundersen G G 2006 Generation of noncentrosomal microtubule arrays *J. Cell Sci.* **119** 4155
[80] Muroyama A and Lechler T 2017 Microtubule organization, dynamics and functions of differentiated cells *Development* **144** 3012
[81] Karplus M 2010 Dynamical aspects of molecular recognition *J. Mol. Recognit.* **23** 102
[82] Bizzarri A R and Cannistraro S ed 2012 *Dynamic Force Spectroscopy and Biomolecular Recognition* (Boca Raton, FL: CRC Press)
[83] Yusko E C and Asbury C L 2014 Force is a signal that cells cannot ignore *Mol. Biol. Cell* **25** 3717–25
[84] Sarangapani K K and Asbury C L 2014 Catch and release: how do kinetochores hook the right microtubules during mitotis? *Trends Genet.* **30** 150
[85] Chen Y, Ju L, Rushdi M, Ge C and Zhu C 2017 Receptor-mediated cell mechanosensing *Mol. Biol. Cell* **28** 3134–55
[86] Niklas R B 1997 How cells get the right chromosomes *Science* **275** 632–7
[87] Musachhio A and Salmon E D 2007 The spindle-assembly checkpoint in space and time *Nat. Rev. Mol. Cell Biol.* **8** 379–93
[88] Brockman J M and Salaita K 2019 Mechanical proofreading: a general mechanism to enhance the fidelity of information transfer between cells *Frontiers Phys.* **7** 1–9
[89] Dumont S and Prakash M 2014 Emergent mechanics of biological structures *Mol. Biol. Cell* **25** 3461–5
[90] Elting M W, Suresh P and Dumont S 2018 The spindle: integrating architecture and mechanics across scales *Trends Cell Biol.* **28** 896–910
[91] Reber S and Hyman A A 2015 Emergent properties of the metaphase spindle *Cold Spring Harbor Perspect. Biol.* **7** a015784
[92] Kapitein L C, Janson M E, van den Wildenberg S M J L, Hoogenraad C C, Schmidt C F and Peterman E J G 2008 Microtubule-driven multimerization recruits ase1p onto overlapping microtubules *Curr. Biol.* **18** 1713
[93] Valentine M T, Fordyce P M, Krzysiak T C, Gilbert S P and Block S M 2006 Individual dimers of the kinesin motor eg5 step processively and support substantial loads *in vitro Nat. Cell Biol.* **8** 470

[94] Shtylla B and Keener J P 2011 A mathematical model for force generation at the kinetochore-microtubule interface *SIAM J. Appl. Math.* **71** 1821

[95] Waters J C, Mitchison T J, Rieder C L and Salmon E D 1996 The kinetochore microtubule minus-end disassembly associated with poleward flux produces a force that can do work *Mol. Biol. Cell.* **7** 1547

[96] Valentine M T, Fordyce P M and Block S M 2006 Eg5 steps it up! *Cell Div.* **1** 31

[97] Marshall W F, Marko J F, Agard D A and Sedat J W 2001 Chromosome elasticity and mitotic polar ejection force measured in living Drosophila embryos by four-dimensional microscopy-based motion analysis *Curr. Biol.* **11** 569